

AD-785 263

**DIFFERENTIAL CAPACITANCE STUDY ON THE
EDGE ORIENTATION OF PYROLYtic GRAPHITE
AND GLASSy CARBON ELECTRODES**

Jean-Paul Randin, et al

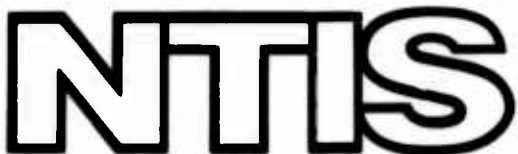
Case Western Reserve University

Prepared for:

Office of Naval Research

1 July 1974

DISTRIBUTED BY:



**National Technical Information Service
U. S. DEPARTMENT OF COMMERCE
5285 Port Royal Road, Springfield Va. 22151**

AD 785 263

DOCUMENT CONTROL DATA - R & D

(Security classification of title, body of abstract and indexing annotation must be entered when the overall report is classified)

1. ORIGINATING ACTIVITY (Corporate author) Case Western Reserve University Cleveland, Ohio 44106		2a. REPORT SECURITY CLASSIFICATION Unclassified
		2b. GROUP -----
3. REPORT TITLE DIFFERENTIAL CAPACITANCE STUDY ON THE EDGE ORIENTATION OF PYROLYTIC GRAPHITE AND GLASSY CARBON ELECTRODES		
4. DESCRIPTIVE NOTES (Type of report and inclusive dates) Technical Report 38		
5. AUTHOR(S) (First name, middle initial, last name) Jean-Paul Randin and Ernest Yeager		
6. REPORT DATE 1 July 1974	7a. TOTAL NO. OF PAGES 24 29	7b. NO. OF REFS 24
8a. CONTRACT OR GRANT NO. N00014-67-A-0404-0006	9a. ORIGINATOR'S REPORT NUMBER(S) Technical Report	
b. PROJECT NO. NR 359-451	9b. OTHER REPORT NO(S) (Any other numbers that may be assigned this report)	
c.		
d.		
10. DISTRIBUTION STATEMENT Approved for Public Release; Distribution Unlimited		
11. SUPPLEMENTARY NOTES ---	12. SPONSORING MILITARY ACTIVITY Office of Naval Research Arlington, Virginia 22217 Code 472: Chemistry Program	
13. ABSTRACT The differential electrode capacitance of the edge orientation (plane perpendicular to the basal one) of stress-annealed pyrolytic graphite and glassy carbon have been studied in concentrated aqueous solutions using an a.c. impedance bridge. The salient features are as follows: <ol style="list-style-type: none"> 1. The apparent differential capacity for the edge orientation of stress-annealed pyrolytic graphite is much higher than on the basal plane because of higher surface roughness and capacitive contribution of the surface groups. The capacity strongly depends on the electrolyte, pH and potential scan range and exhibits a complex potential dependence, probably as a result of the specific chemical groups on the surface. A model is proposed to explain the behavior of the edge orientation. 2. The capacity minimum for the glassy carbon is sufficiently low so as to suggest a space charge contribution from within the electrode phase. 3. The similarities between the potential dependence of the capacity for the edge orientation of pyrolytic graphite and glassy carbon indicate similarity in the surface groups although the particular groups cannot be specifically identified from the electrochemical measurements. 		

Reproduced by
NATIONAL TECHNICAL
INFORMATION SERVICE
U.S. Department of Commerce
Springfield, VA 22151

DD FORM 1 NOV 68 1473

Unclassified

Security Classification

Unclassified

Security Classification

14. KEY WORDS	LINK A		LINK B		LINK C	
	ROLE	WT	ROLE	WT	ROLE	WT
graphite electrodes						
glassy carbon						
semiconductors						
electrochemical capacity						
space charge regions						

Unclassified

Security Classification

OFFICE OF NAVAL RESEARCH

Contract N00014-67-A-0404-0006

Project NR 359-451

TECHNICAL REPORT NO. 38

DIFFERENTIAL CAPACITANCE STUDY ON THE EDGE
ORIENTATION OF PYROLYTIC GRAPHITE AND
GLASSY CARBON ELECTRODES

by

Jean-Paul Randin * and Ernest Yeager

Prepared for Publication

in the

Journal of Electroanalytical Chemistry

Department of Chemistry
CASE WESTERN RESERVE UNIVERSITY
Cleveland, Ohio 44106

1 July 1974

Reproduction in whole or in part is permitted for any
purpose of the United States Government

This document has been approved for public release and sale;
its distribution is unlimited.

* Present address: Hydro-Quebec Institute of Research
Varennes, P.Q., Canada

TABLE OF CONTENTS

TITLE PAGE	i
DOCUMENT CONTROL DATA - R & D	ii
TABLE OF CONTENTS	iv
LIST OF FIGURES	v
ABSTRACT	1
INTRODUCTION	2
EXPERIMENTAL	3
RESULTS	
1. Edge orientation of stress-annealed pyrolytic graphite	4
2. Glassy carbon	6
DISCUSSION	7
ACKNOWLEDGEMENT	12
REFERENCES	13
DISTRIBUTION LIST	23

LIST OF FIGURES

Figure 1 Capacity-potential curves for the edge orientation of stress-annealed pyrolytic graphite in 0.9 N NaF (pH=6) at 25°C and 1000 Hz, without hood. Initial scan anodic starting at point S.

— potentials going positive
--- potentials going negative from -0.1 V
— potentials going negative from +0.2 V
-.-.- potentials going negative from +0.5 V
..... potentials going negative from +0.8 V

Figure 2 Capacity-potential curves for the edge orientation of stress-annealed pyrolytic graphite in 1N H₂SO₄ and 1N NaOH at 25°C and 1000 Hz, without hood.

A) 1 N H₂SO₄ — potentials going positive
--- potentials going negative from +0.1 V
-.-.- potentials going negative from +0.4 V
..... potentials going negative from +0.8 V

B) 1 N NaOH — potentials going positive
--- potentials going negative from -0.4 V
-.-.- potentials going negative from -0.2 V
..... potentials going negative from +0.2 V

Figure 3 Current-potential curves for the edge orientation of stress-annealed pyrolytic graphite at 25°C, without hood. Scan rate 0.1 V/sec, direction of sweep indicated by arrows. Different curves for the same electrolyte differ in the range of potential of scans.

A) in 1 N H₂SO₄; B) in 0.9 N NaF, pH = 6; C) in 1 N NaOH

Figure 4 Capacity-potential curves for the glassy carbon in 0.9 N NaF (pH = 6) at 25°C and 1000 Hz, with hood.

— potentials going positive
--- potentials going negative from -0.1 V
- - - potentials going negative from +0.2 V
-.-.- potentials going negative from +0.5 V
..... potentials going negative from +0.8 V

Figure 5 Capacity-potential curves for the glassy carbon in 1 N H₂SO₄ and 1 N NaOH at 25°C and 1000 Hz, with hood.

A) 1 N H_2SO_4 ——— potentials going positive
 --- potentials going negative from +0.05 V
 - - - potentials going negative from +0.4 V
 -.-.- potentials going negative from +0.8 V
 potentials going negative from +1.25 V

B) 1 N NaOH ——— potentials going positive
 --- potentials going negative from -0.4 V
 - - - potentials going negative from -0.2 V
 -.-.- potentials going negative from 0.0 V
 potentials going negative from +0.3 V

Figure 6 Current-potential curves for the glassy carbon at 25°C, with hood. Scan rate 0.1 V/sec, direction of sweep indicated by arrows.

A) in 1 N H_2SO_4 ; B) in 0.9 N NaF, pH = 6; C) in 1 N NaOH

Figure 7 Model for the surface of the edge orientation of stress-annealed pyrolytic graphite in arbitrary unit. The space charge region within the graphite electrode is represented by the dashed line.

Figure 8 Distributive impedance for a fissured or porous electrode in the absence of faradaic components. R_0 - resistance of bulk electrolyte; R_1 , R_i - resistance of electrolyte in fissures or pores; C - interfacial capacitance.

DIFFERENTIAL CAPACITANCE STUDY ON THE EDGE ORIENTATION
OF PYROLYTIC GRAPHITE AND GLASSY CARBON ELECTRODES

Jean-Paul Randin* and Ernest Yeager

Department of Chemistry
CASE WESTERN RESERVE UNIVERSITY
Cleveland, Ohio 44106

ABSTRACT

The differential electrode capacitance of the edge orientation (plane perpendicular to the basal one) of stress-annealed pyrolytic graphite and glassy carbon have been studied in concentrated aqueous solutions using an a.c. impedance bridge. The salient features are as follows:

- 1) The apparent differential capacity for the edge orientation of stress-annealed pyrolytic graphite is much higher than on the basal plane because of higher surface roughness and capacitive contribution of the surface groups. The capacity strongly depends on the electrolyte, pH and potential scan range and exhibits a complex potential dependence, probably as a result of the specific chemical groups on the surface. A model is proposed to explain the behavior of the edge orientation.
- 2) The capacity minimum for the glassy carbon is sufficiently low so as to suggest a space charge contribution from within the electrode phase.
- 3) The similarities between the potential dependence of the capacity for the edge orientation of pyrolytic graphite and glassy carbon indicate similarity in the surface groups although the particular groups cannot be specifically identified from the electrochemical measurements.

* Present address: Hydro-Quebec Institute of Research
Varennes, P.Q., Canada

INTRODUCTION

In previous publications (1-2), the non-faradaic differential capacity measured on the basal plane of high-pressure, stress-annealed pyrolytic graphite has been reported to have a near parabolic dependence on electrode potential with a minimum of about $3 \mu\text{F cm}^{-2}$ in concentrated electrolytes. This low capacity value compared favorably with that estimated from the carrier concentration using the presently available theory of the space charge layer in semiconductor electrodes. Studies in NaF solutions at concentrations as low as 10^{-5} N indicated that in the range of potential studied (0.5 to -0.5 V vs NHE) this minimum in the capacity vs. potential curve was not associated with a corresponding minimum in the capacity of the diffuse ionic layer. A.c. impedance measurements have also been made on boronated stress-annealed pyrolytic graphite (3). The direction of the shift in the capacity minimum is in agreement with the semiconductor interpretation but the magnitude of the shift is much larger and the capacity of the minimum substantially lower than estimated theoretically from the carrier concentration.

The present paper involves the study of the differential capacitance on the edge orientation (plane perpendicular to the basal plane) of the stress-annealed pyrolytic graphite to establish the extent to which the surface chemistry influences the capacity. Capacitance measurements for glassy carbon have also been carried out. This material is prepared by carbonization and subsequent thermal treatment of organic materials. This carbon is characterized by isotropy of properties, high purity, strength and

hardness, and extremely low permeability to both gases and liquids. Chemical properties are, generally speaking, those of carbon, but with a much reduced activity at least in part because of a low porosity. Its structure has been the object of several studies which have been reviewed recently (4). The accepted model involves the presence of two types of carbon atoms, one involving trigonal (sp^2) bonding and the other having tetrahedral (sp^3) bonding. The relative amount of trigonal carbon atoms depends on the heat treatment. A semiconductor model has been proposed for glassy carbon (5) with a very small energy gap of approximately 10^{-2} to 10^{-3} eV. The carrier concentration in glassy carbon depends on the heat treatment temperature in the preparation of the sample. For samples prepared at 2000°C , the carrier concentration has been reported to be $2 \cdot 10^{20}$ carriers cm^{-3} with n-type conductivity and $0.9 \cdot 10^{20}$ carriers cm^{-3} at 3000°C with p-type conductivity (5).

EXPERIMENTAL

The stress-annealed pyrolytic graphite used in this study^{a)} was the same as used previously (1) and had an X-ray rocking curve whose mosaic spread width is approximately 0.3 to 0.4° at half-intensity of the (002) diffraction line. Because of the fragile nature of this material in the edge orientation, the electrodes with this orientation exposed to the electrolyte were prepared by compression moulding (6) within a Kel-F holder rather than press-fitted into Teflon as was mounted the basal plane (1). The exposed section of these edge orientation electrodes was approximately square with an area of $\sim 0.2 \text{ cm}^2$. The glassy carbon electrode^{b)} was prepared from a 6mm diameter rod, press-fitted coaxially into a cylindrical Teflon holder.

a) Supplied by the Union Carbide Technical Center Research, Parma, Ohio 44130

b) Gallard-Schlesinger Chemical Mfg. Corp., Carle Place, N.Y.

Before each electrochemical measurement, the electrodes were mechanically polished using different grades of alumina down to AB gamma (0.05μ , Buehler Ltd). Polishing was done in the presence of conductivity water. The abrasive was subsequently removed by washing thoroughly the electrode with conductivity water. The electrode was then kept wet until slipped into the electrolyte.

The electrochemical system, the purifications of electrolytes and gas, and the instrumentation used in this study were described previously (1). All measurements were performed at $\sim 25^\circ\text{C}$. Unless otherwise indicated the potentials are given with respect to a normal hydrogen electrode (NHE). All capacitances are given in terms of apparent electrode area.

RESULTS

1. Edge orientation of stress-annealed pyrolytic graphite

In the earlier work on the basal plane (1-3) a Teflon hood, slipped over the electrode assembly, greatly reduced frequency dispersion of the measured capacity by providing more uniform current distribution on the electrode. It was essential however that the electrolyte not penetrate between the Teflon of the hood and the masked portion of the electrode surface. Unfortunately, with the edge orientation of stress-annealed pyrolytic graphite, electrolyte penetration could not be prevented and hence appreciable frequency dispersion was found even with the hood. Further, the hood tended to damage the electrode surface where it made contact with it. The difference in the frequency dependence of the capacity

measured with and without the hood was not very large. For example, with the hood the frequency dispersion was approximately 8% per decade and without the hood approximately 15%. In view of the disadvantage of using the hood, further measurements on the edge orientation were performed without it.

The capacity-potential curves on the edge orientation of stress-annealed pyrolytic graphite in 0.9N NaF are reported in Fig. 1. The individual points are not shown. The point-by-point measurements were made with ~ 50 mV separation with each measurement requiring approximately 1-2 minutes. The values recorded with increasing anodic potentials do not depend on the anodic potential applied during the previous scans, provided the starting potential was cathodic enough to generate a reduced surface. In contrast, the shape of the cathodic scan depends on the maximum anodic potential reached during the preceding anodic scan. The hysteresis between an anodic scan and the subsequent cathodic scan is more pronounced, the more anodic the potential reached before reversing the direction of the scan.

The shape of the capacity-potential curves (Fig. 2) depends strongly on the electrolyte. In 1 N H_2SO_4 the relative variations of capacity with the electrode potential are much more pronounced than in 1 N NaOH (Fig. 2). The minimum value in the capacity-potential curve, as well as the potential at which it occurs, depends on pH in a rather complex manner. In the acid part of the curve, the potential of the minimum changes about -30 mV/pH, whereas in alkaline solutions the dependence is close to -60 mV/pH.

The corresponding voltammetry curves for the edge orientation (Fig. 3) show rather broad ill-defined irreversible peaks. The capacitance calculated from these curves is far higher than from the a.c. capacity measurements. For example, for the NaF solution at 0 V vs NHE the capacity from the voltammetry curve is $\sim 750 \mu\text{F cm}^{-2}$ apparent area. Further, at much lower sweep rates the capacity is even higher; for example, at the same potential for 0.01 V/sec, the capacity is $\sim 3000 \mu\text{F cm}^{-2}$. The peak observed at about +0.6 V vs RHE in the anodic sweep of the linear sweep voltammetry has a pH dependence with a slope of about -60 mV/pH (Fig. 3).

2. Glassy carbon

The frequency dependence of the capacity on the glassy carbon exhibits a behavior comparable to that observed on the edge orientation of stress-annealed pyrolytic graphite. Since no practical problem was associated with slipping the Teflon hood on to the glassy carbon electrode, it was used in all measurements performed with this material. The hood was slipped on to the polished electrode under water and, then, the electrode was transferred immediately into the electrolyte within the electrochemical cell, while always under conductivity water.

The capacity-potential curves measured on the glassy carbon electrode in 0.9 N NaF ($\text{pH} \approx 6$), in 1N H_2SO_4 , and in 1N NaOH are shown in Figs. 4 and 5. As for the edge orientation, the shape of the reverse cathodic scan depends on the maximum positive potential reached in the preceding anodic scan. In the case of the glassy carbon, the shape of the capacity-potential curve and the absolute values of the capacity are

even more pH dependent than for the edge orientation of pyrolytic graphite. The minimum capacity is three times higher in alkaline solutions than in acid media. The peak previously observed for the edge orientation in acid media at about +0.6 V vs. RHE on the cathodic sweep is also observed for the glassy carbon at about the same potential. This peak is very well defined in acid media but is not distinguishable any more in alkaline solutions (Fig. 5). The pH dependence of the electrode potential at the minimum capacity has a slope of about -30 mV/pH over the whole pH range from ~ 0 to ~ 14.

The voltammetry curves for the glassy carbon again have broad ill-defined irreversible peaks (Fig. 6). The capacities calculated from the voltammetry curves are also very large compared to the a.c. capacities.

DISCUSSION

The main features of the present study are as follows: first, the capacity of the edge orientation on stress-annealed pyrolytic graphite is much higher than on the basal plane and is strongly dependent on the electrolyte, pH and potential scan range; secondly, the capacity has a complex potential dependence, probably as a result of the specific chemical groups on the surface which contribute to the capacity through changes in their oxidation state or state of ionization. The relatively high a.c. capacity can be due to surface roughness or to the capacitive contribution of the surface groups or both. The capacities calculated from the voltammetric curves are equivalent to very low frequency values. A comparison of these values at different sweep rates, together with the a.c. impedance data,

indicates that the capacity increases very drastically at very low frequencies.

Two possible explanations for this increment in capacity are 1) the presence of surface microfissures (Fig. 7) and 2) slow surface states involving various chemical groups on the edge surface. Electrolyte can penetrate into surface fissures and give rise to a distributed impedance network as shown in Fig. 8 with the resistance components corresponding to electrolyte resistance. The width of these fissures may be as small as 10^{-7} cm and still permit ion migration. An attempt has been made to represent the space charge region within the graphite electrode with the dashed line in Fig. 7. Even though the capacity associated with the basal plane within the fissures is still small per unit true area, the large area leads to a large surface capacity but only at frequencies sufficiently low for the capacitive components in the distribution network (Fig. 8) to be predominant.

While the distributive impedance model is a valid approach to the description of the electrode impedance, it is doubtful that this accounts for the majority of the order of magnitude increments in capacity at very low frequencies. No significant series resistance component was noted in the measurements with either the edge orientation or the glassy carbon, beyond that associated with bulk electrolyte. Further almost as large an increment in capacity was found with glassy carbon which is relatively non-porous.

Consequently the more likely explanation for this increment in capacity at low frequencies is slow surface states involving changes in the oxidation state of the electrode surface which are far too slow to contribute to the observed capacitance at the frequencies involved in the a.c. impedance measurements. The oxidation-reduction of other surface functional groups, however, may be sufficiently reversible so as to still contribute substantially to the capacity at audio frequency and cause

the complex capacity-potential behavior found in the present work.

Normally surface states associated with a specific functional group should contribute to the capacity only over a relatively narrow potential range. If there is a wide distribution of functional groups with strong interactions, however, their contribution to the capacity may be large over a wide range of potentials with a complex potential dependence. The pH dependence of these surface state contributions to the a.c. capacitance arises from the pH dependence of the oxidation and ionization states of these functional groups (usually -30 or -60 mV/pH for double or single charge-transfer processes).

The similarity between some features of the potential dependence of the differential capacity of both the edge orientation of pyrolytic graphite and glassy carbon is rather surprising considering the different structures of the two electrode materials. This may indicate that similar surface groups are probably present at both electrode surfaces.

In contrast with the behavior of the basal plane, the minimum in the capacity-potential curve depends on pH for the edge orientation as well as for the glassy carbon. Pronounced pH dependence of the capacity minimum is found with most semiconductor electrodes including germanium (7-9) and is associated with the presence of surface groups whose state of charge is pH dependent. The explanation for the apparent shift of the flat band potential for the edge orientation of graphite and the glassy carbon is probably similar to that proposed by Gerischer et al. (8) for germanium. A redistribution of charge occurs between the electrode surface and the outer Helmholtz plane as a consequence of the ionization of surface functional groups whose ionization constants depend on the oxidation state. The basal plane of graphite is rather unique in not having such

groups and therefore a pH independent flat band potential.

The problem of functional groups of graphite and carbon electrodes is beyond the scope of this publication. A brief account of previous studies on the surface chemistry of graphite, however, is relevant to the present study. The nature of the functional groups on surfaces of different kinds of carbons and graphite has been extensively studied and the subject of several reviews (10-12,24). On micro-crystalline carbons (i.e., amorphous carbon, active carbons, carbon blacks, carbon brushes, cokes) a large variety of surface groups have been identified. On graphite, most chemical reactions on the surface are difficult to observe because of the extremely small quantity available due to the low specific surface area. The formation of surface oxides on the edge orientation of graphite single crystal was first shown by Hennig (13) and later confirmed by Montet (14). Recently, Thomas *et al.* (15), using x-ray photoelectron spectroscopy (ESCA), have detected from the oxygen 1s peak the chemisorption of oxygen at the edge orientation of stress-annealed pyrolytic graphite. The width of the peak indicates that at least two types of chemical linkages exist for the bound oxygen. Spectra obtained on the basal surfaces show no peak in the high resolution scan at the region of binding energy corresponding to oxygen 1s, confirming the inertness of this surface. The stress-annealed pyrolytic graphite studied by Thomas *et al.* (15) was from the same origin as that used in the present work.

Tarasevich *et al.* (16) have recently published voltammetry curves for ordinary pyrolytic graphite which are basically the same as obtained in the present work (Fig. 3). [Voltammetric studies of graphite and carbon electrodes have also been published recently (17,18).] Various workers including Garten and Weiss (19) and Epstein *et al.* (20) have suggested that the oxidized and reduced forms of the surface functional groups

observed electrochemically on graphite and carbon correspond to the quinone/hydroquinone couple, but the chromene-carbonium ion couple also has been proposed (21).

Although oxidation-reduction potentials are not sufficient to identify a functional group, comparison of the experimental potentials with the peaks in the a.c. capacity curves with some known oxido-reduction potentials for organic couples are of interest. Several oxidation-reduction potentials of organic compounds (for example: quinone-hydroquinone, $E_o = 0.6995$ V at 25°C; 1,2-naphthoquinone, $E_o = 0.547$ V at 25°C (22)) fall in the potential range of the peak observed in the capacity-potential curves around 0.6 V vs. RHE. The quinone-hydroquinone surface group is a likely expectation but no strong evidence is available in the present study to support this hypothesis.

The capacity minimum for the glassy carbon is sufficiently low so as to suggest a space charge contribution from within the electrode phase even assuming no surface roughness. If we proceed to calculate a space charge capacitance with the same assumptions and equations used in ref. 1, the value comes out to be: $\sim 13 \mu\text{F cm}^{-2}$. This calculation has been carried out using 3 for the dielectric constant (23) and 10^{19} cm^{-3} for the carrier concentration (5) assuming an intrinsic semiconductor. Assuming a Helmholtz capacity of $20 \mu\text{F cm}^{-2}$, this calculation leads to a predicted capacity of $\sim 8 \mu\text{F cm}^{-2}$, as compared to an observed minimum value of $\sim 10 \mu\text{F cm}^{-2}$ in 1N H_2SO_4 . The apparent agreement between the rough calculation and the experimental value is probably fortuitous because of the many assumptions that are involved in the theoretical calculations.

ACKNOWLEDGEMENT

The authors are pleased to acknowledge the support of this research by the U.S. Office of Naval Research. One of us (J.-P.R.) thanks the Stiftung für Stipendien auf dem Gebiete der Chemie, Basel, Switzerland, for the award of a Research Fellowship. The authors also express appreciation to the Union Carbide Technical Center, Parma, Ohio and Dr. A. Moore of that laboratory for providing the stress-annealed pyrolytic graphite used in this study.

REFERENCES

1. J.-P. Randin and E. Yeager, *J. Electroanal. Chem.* 36, 257 (1972).
2. J.-P. Randin and E. Yeager, *J. Electrochem. Soc.* 118, 711 (1971).
3. J.-P. Randin and E. Yeager, *J. Electroanal. Chem.*, submitted for publication.
4. T. Noda, M. Inagaki and S. Yamada, *J. Non-Crystalline Solids*, 1, 285 (1969).
5. T. Tsuzuku and K. Saito, *Japan J. Appl. Phys.* 5, 738 (1966).
6. D. Yohe, E. Yeager, R. Greef and A. Riga, "Electrochemical Processes on Nickel Oxide", Technical Report No 3, Case Western Reserve University, Cleveland, Ohio, U.S. Office of Naval Research, Contract No 1439 (09); project NR 056-451, July 1, 1967.
7. M. Hoffmann-Perez and H. Gerischer, *Z. Elektrochem.* 65, 771 (1961).
8. H. Gerischer, M. Hoffmann-Perez and W. Mindt, *Ber. Busenges. Physik. Chem.* 69, 130 (1965).
9. H. Gerischer, in "Physical Chemistry, An Advanced Treatise", Vol. IXA, Electrochemistry, (H. Eyring, ed.), Academic Press, New York, 1970, p. 468.
10. H.B. Boehm, in "Advances in Catalysis and Related Subjects", Vol. 16, (D.D. Eley, H. Pines and P.B. Weisz, eds.) Academic Press, New York, 1966, p. 179.
11. J.B. Donnet, *Carbon*, 6, 161 (1968).

12. B.R. Puri, Chem. Phys. Carbon, 6, 191 (1970).
13. G.R. Henning, in "Proc. Fifth Conf. on Carbon", 1, p. 143, Pergamon Press, Oxford (1962).
14. G.L. Montet, in "Proc. Fifth Conf. on Carbon", 1, p. 116, Pergamon Press, Oxford (1962).
15. J.M. Thomas, E.L. Evans, M. Barber and P. Swift, Trans. Faraday Soc. 67, 1875 (1971).
16. M.R. Tarasevich, F.Z. Sabirov, B.I. Lentsner and L.L. Knots, Soviet Electrochemistry, 7, 566 (1971).
17. K.F. Blurton, Electrochim. Acta, 18, 869 (1973).
18. K. Kinoshita and J.A.S. Bett, Carbon, 11, 403 (1973).
19. V.A. Garten and D.E. Weiss, Aust. J. Chem. 8, 68 (1955).
20. B.D. Epstein, E. Dalle-Molle and J.S. Mattson, Carbon, 9, 609 (1971).
21. V.A. Garten and D.E. Weiss, Aust. J. Chem. 10, 309 (1957).
22. W.M. Clark, "Oxidation-Reduction Potentials of Organic Systems", The Williams and Wilkins Co., Baltimore, 1960, p. 356.
23. S. Ergun, J.B. Yasinsky and J.R. Townsend, Carbon, 5, 403 (1967).,
24. V. L. Snoeyink and W. J. Weber, "Surface Function Groups in Carbon and Silica", Progress in Surface and Membrane Science, J. Darielle, M. Rosenberg, and D. Cadenhead, eds., Vol. 5, Chapt. 2, Academic Press, New York, 1972, pp. 63-119.

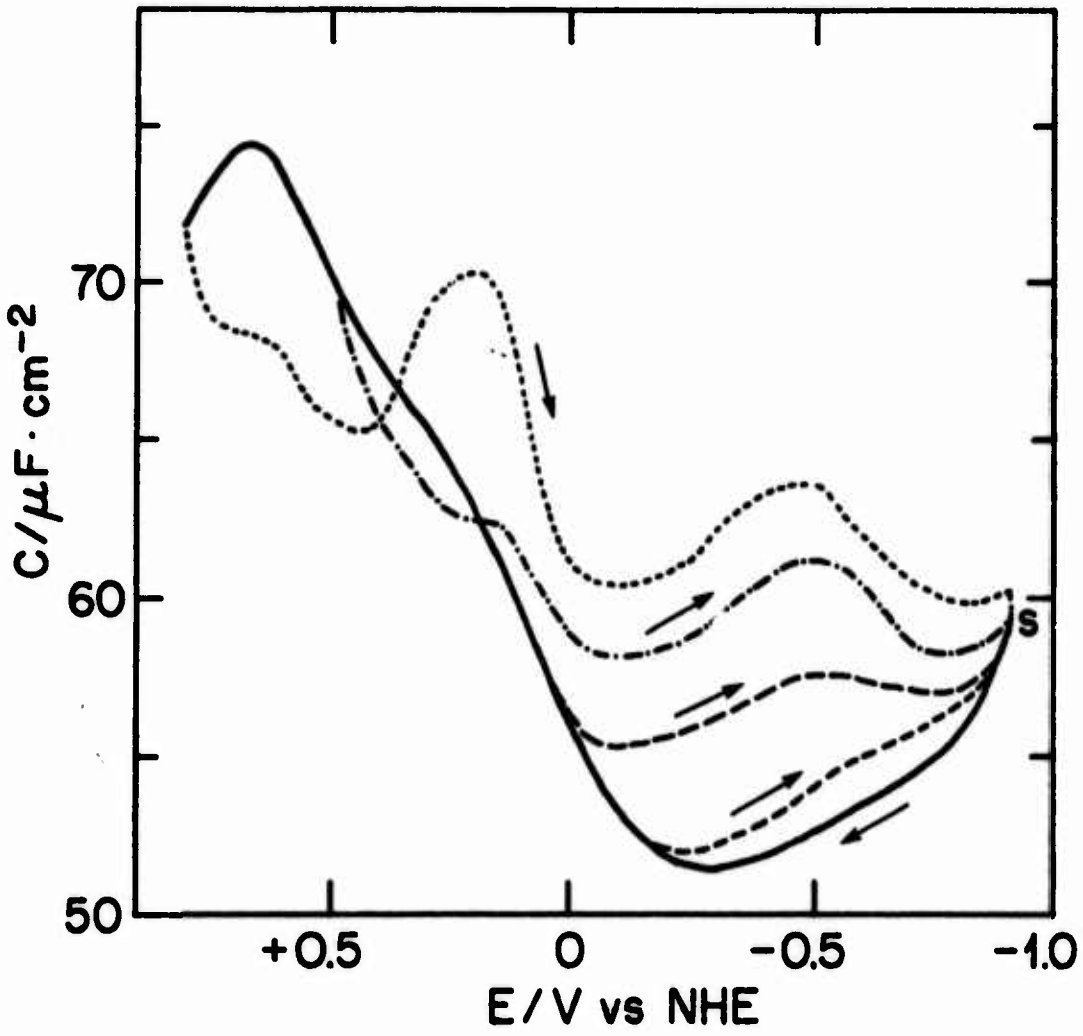


Figure 1 Capacity-potential curves for the edge orientation of stress-annealed pyrolytic graphite in 0.9 N NaF ($\text{pH}=6$) at 25°C and 1000 Hz, without hood. Initial scan anodic starting at point S.

- potentials going positive
- - - potentials going negative from -0.1 V
- - - potentials going negative from +0.2 V
- . - - - potentials going negative from +0.5 V
- potentials going negative from +0.8 V

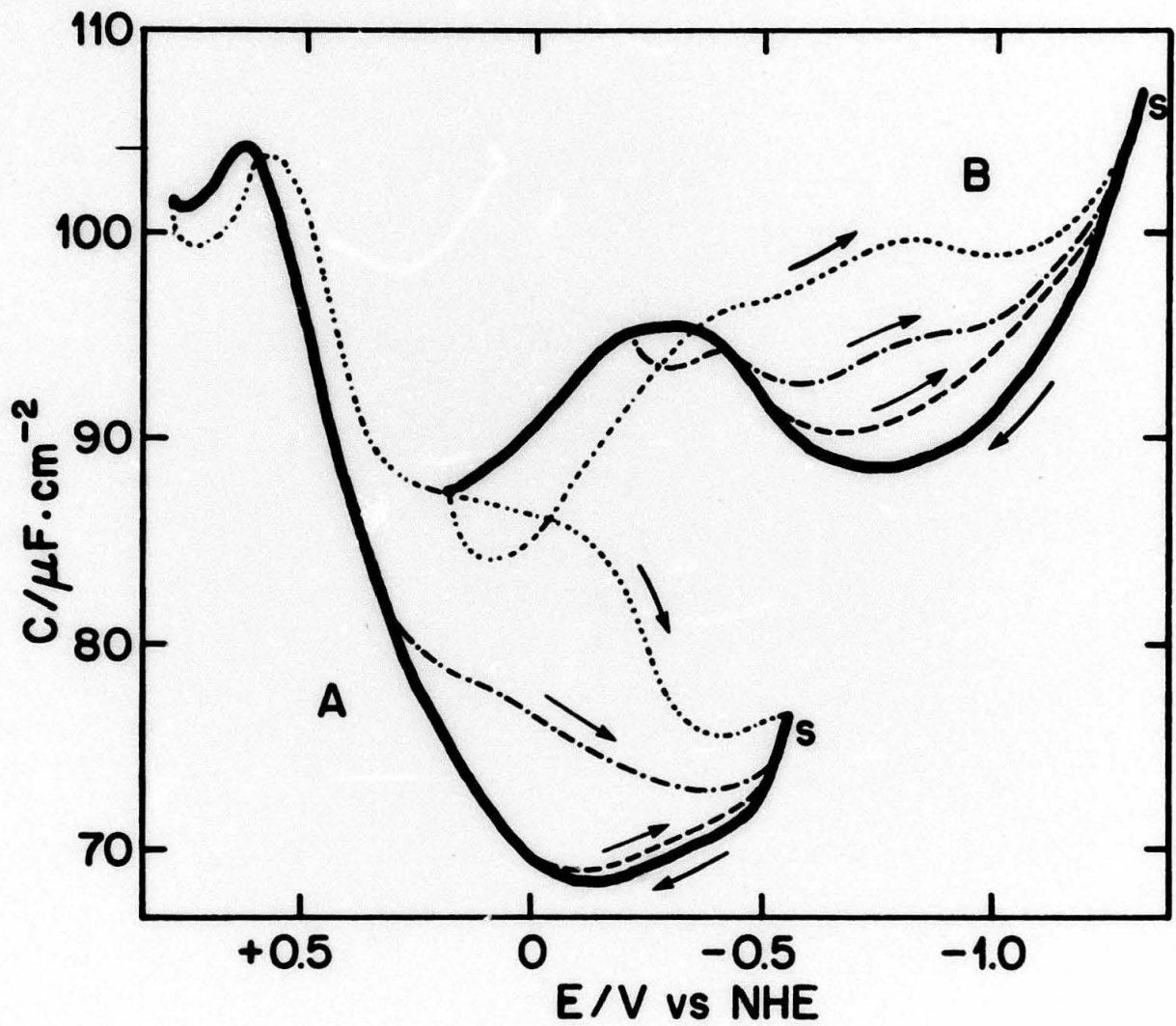


Figure 2 Capacity-potential curves for the edge orientation of stress-annealed pyrolytic graphite in $1\text{N H}_2\text{SO}_4$ and 1N NaOH at 25°C and 1000 Hz, without hood.

A) $1\text{N H}_2\text{SO}_4$

- potentials going positive
- potentials going negative from +0.1 V
- ...-. potentials going negative from +0.4 V
- potentials going negative from +0.8 V

B) 1N NaOH

- potentials going positive
- potentials going negative from -0.4 V
- ...-. potentials going negative from -0.2 V
- potentials going negative from +0.2 V

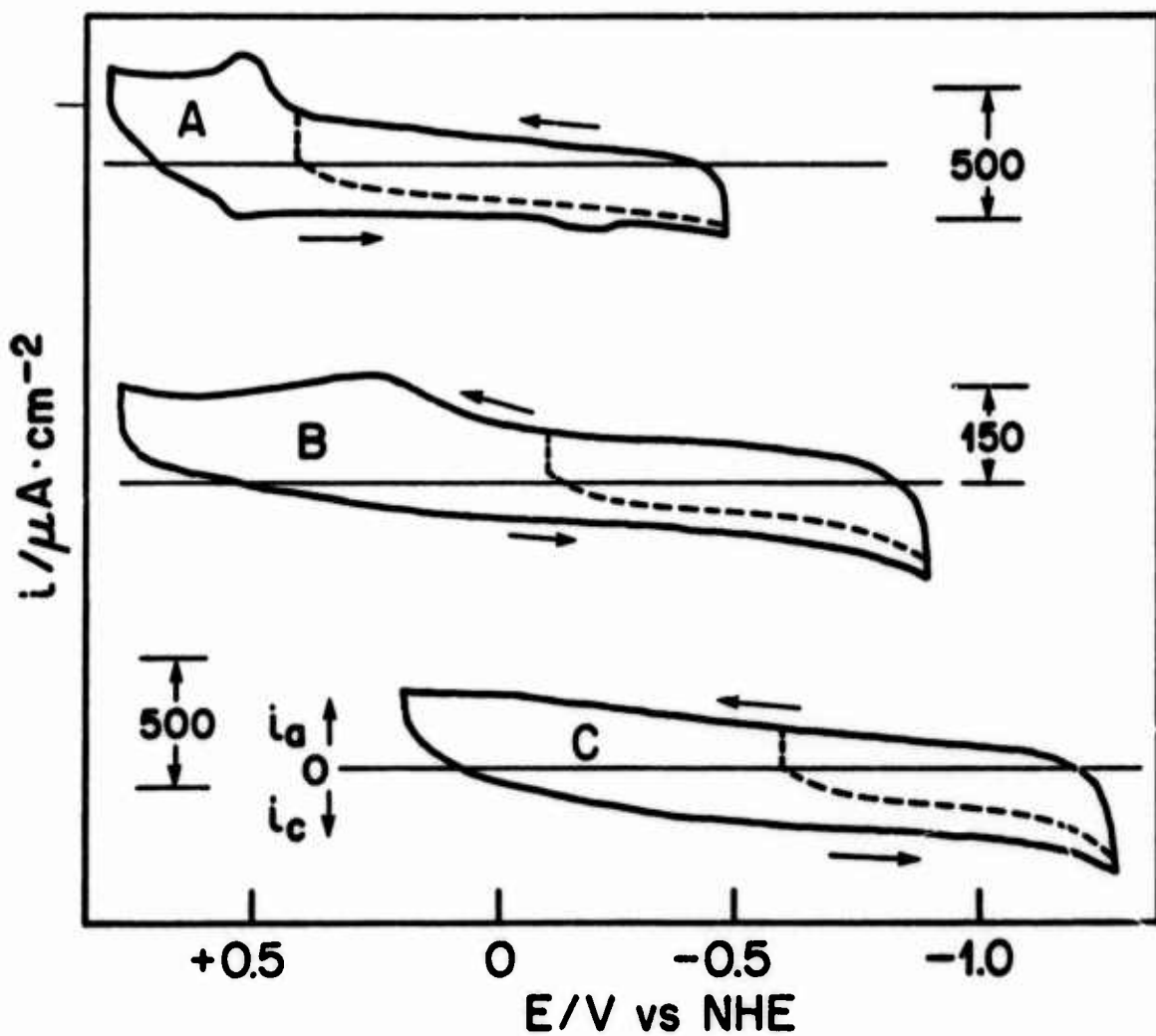


Figure 3 Current-potential curves for the edge orientation of stress-annealed pyrolytic graphite at 25°C, without hood. Scan rate 0.1 V/sec, direction of sweep indicated by arrows. Different curves for the same electrolyte differ in the range of potential of scans.

A) in 1 N H_2SO_4 ; B) in 0.9 N NaF , $\text{pH} \approx 6$; C) in 1 N NaOH

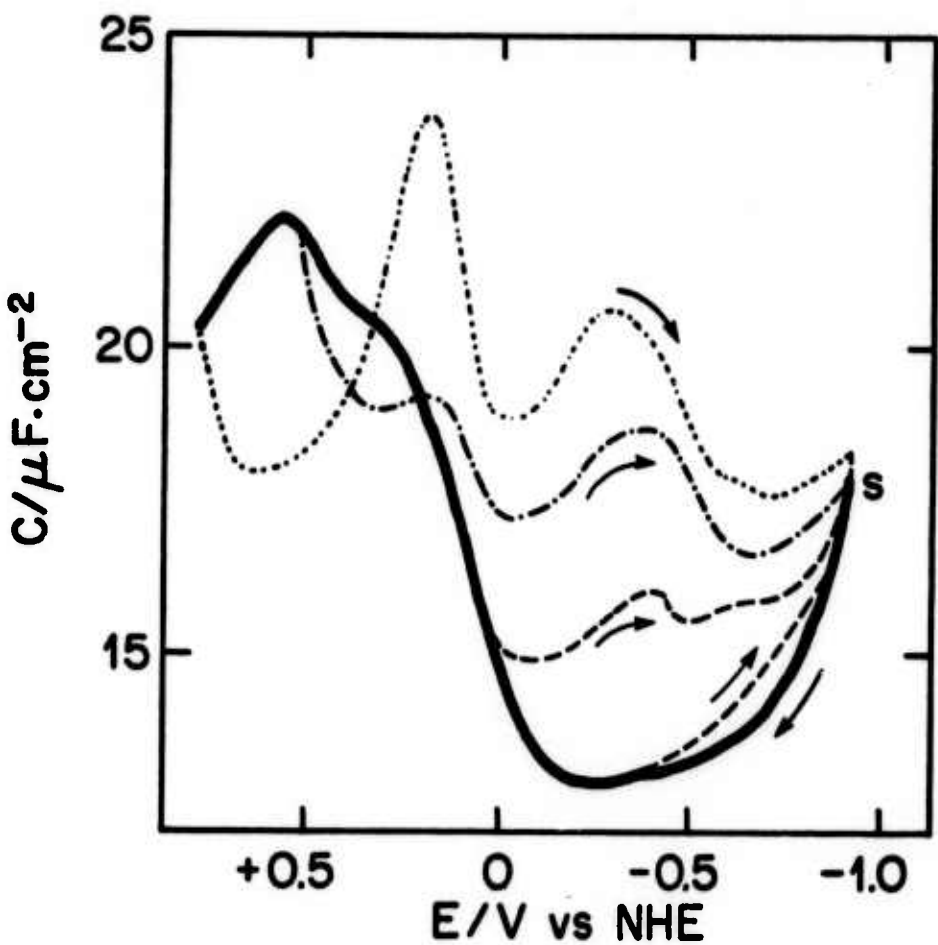


Figure 4 Capacity-potential curves for the glassy carbon in 0.9 N NaF (pH = 6) at 25°C and 1000 Hz, with hood.

- potentials going positive
- potentials going negative from -0.1 V
- - - potentials going negative from +0.2 V
- . - . potentials going negative from +0.5 V
- potentials going negative from +0.8 V

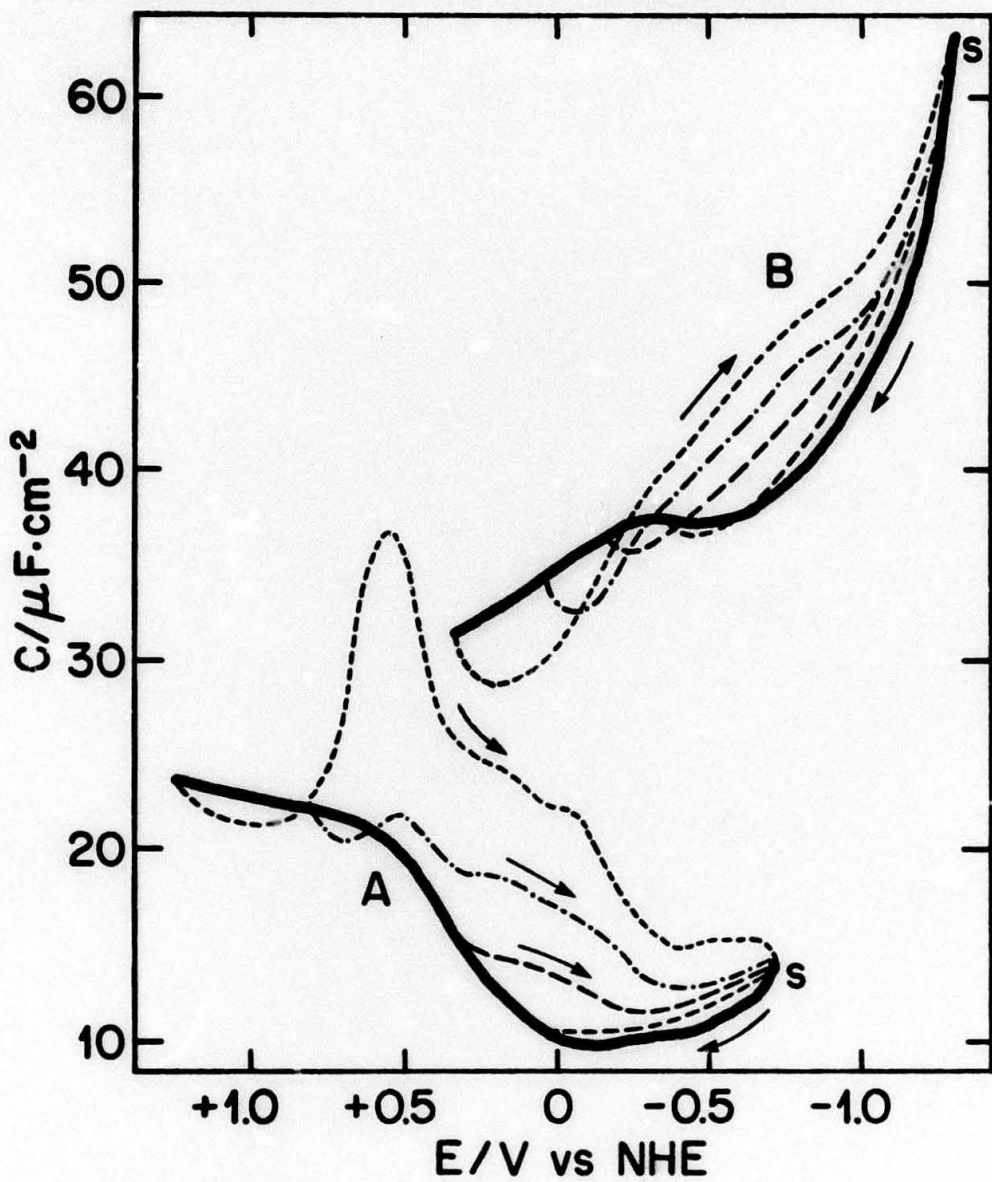


Figure 5 Capacity-potential curves for the glassy carbon in 1 N H_2SO_4 and 1 N $NaOH$ at 25°C and 1000 Hz, with hood.

- A) 1 N H_2SO_4
- potentials going positive
 - potentials going negative from +0.05 V
 - - - potentials going negative from +0.4 V
 - . - . potentials going negative from +0.8 V
 - potentials going negative from +1.25 V
- B) 1 N $NaOH$
- — potentials going positive
 - potentials going negative from -0.4 V
 - - - potentials going negative from -0.2 V
 - . - . potentials going negative from 0.0 V
 - potentials going negative from +0.3 V

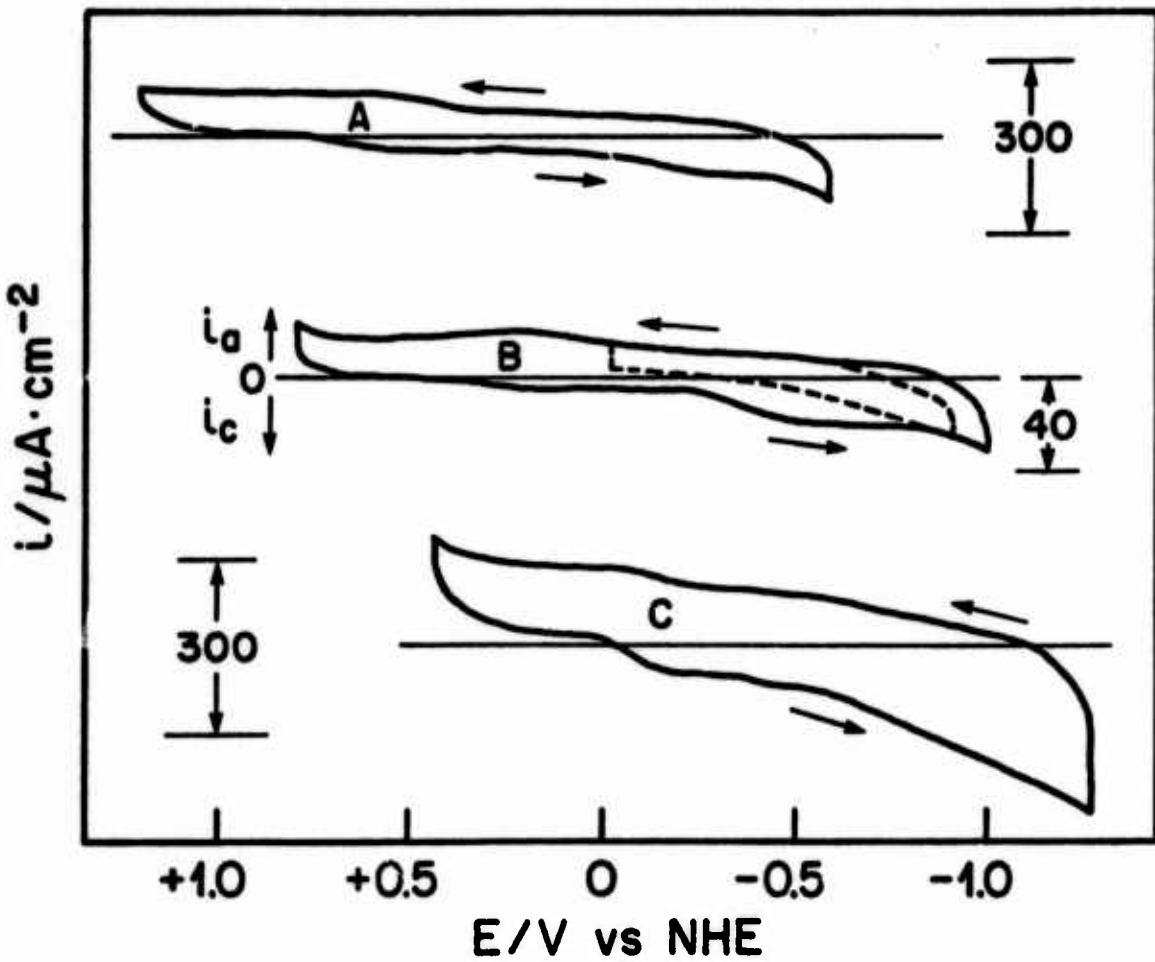


Figure 6 Current-potential curves for the glassy carbon at 25°C , with hood. Scan rate 0.1 V/sec , direction of sweep indicated by arrows.

A) in $1 \text{ N } \text{H}_2\text{SO}_4$; B) in $0.9 \text{ N } \text{NaF}$, $\text{pH} \approx 6$; C) in $1 \text{ N } \text{NaOH}$

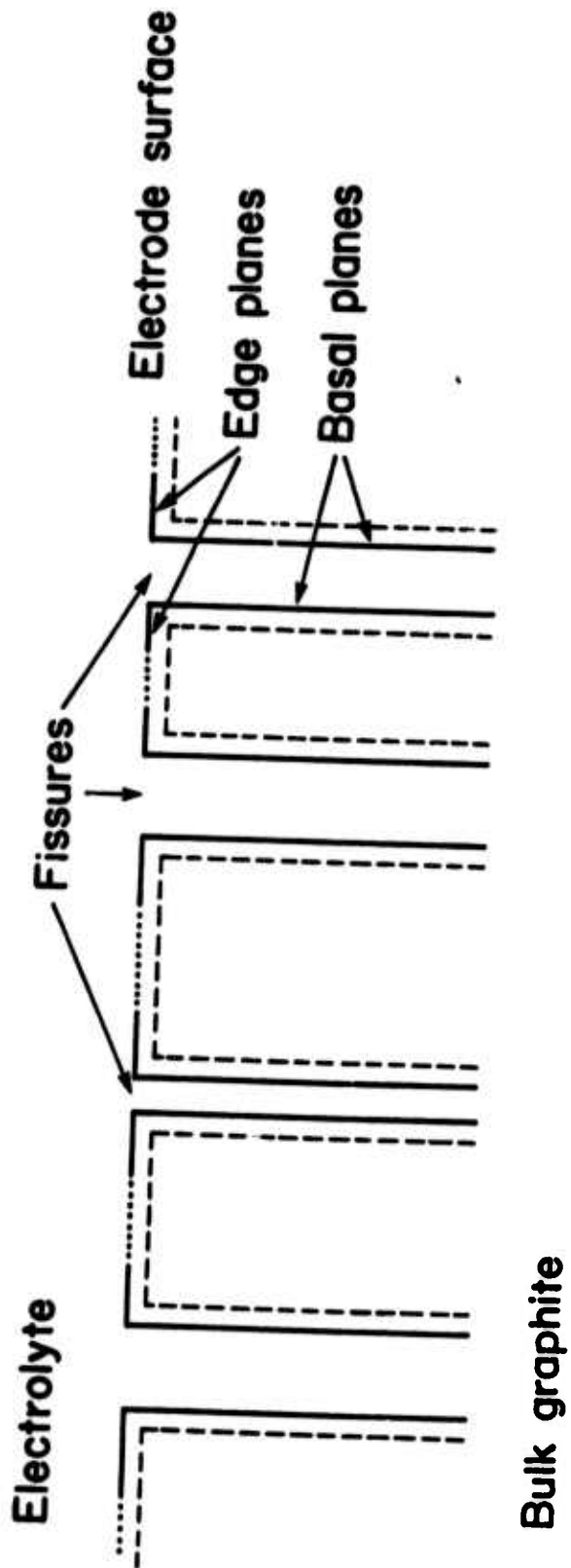


Figure 7 Model for the surface of the edge orientation of stress-annealed pyrolytic graphite in arbitrary unit. The space charge region within the graphite electrode is represented by the dashed line.

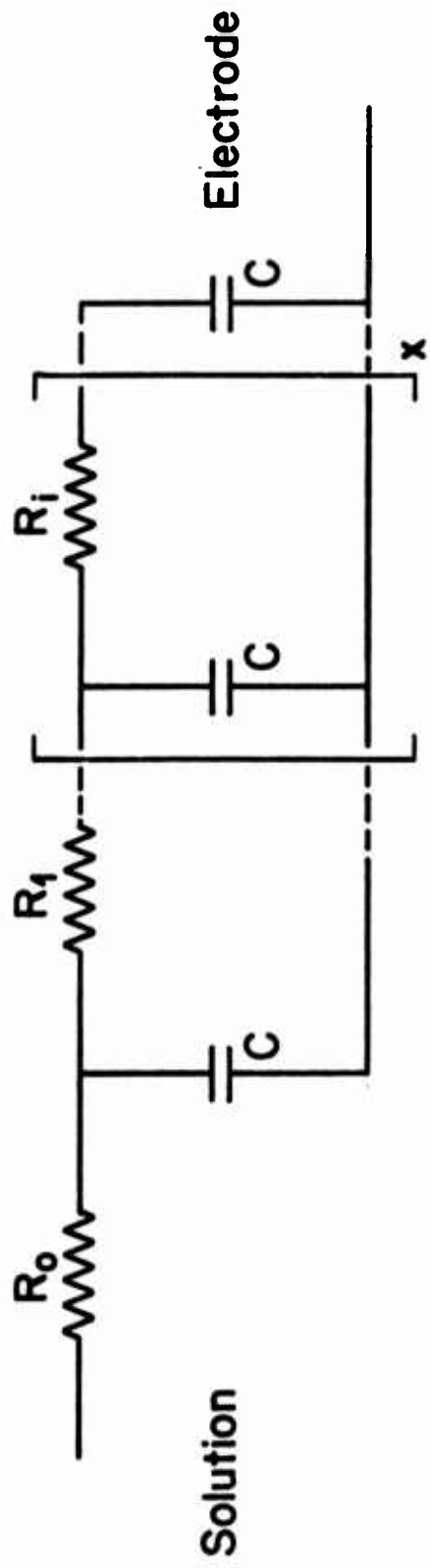


Figure 8 Distributive impedance for a fissured or porous electrode in the absence of faradaic components. R_o - resistance of bulk electrolyte; R_1 , R_i - resistance of electrolyte in fissures or pores; C - interfacial capacitance.